6024 *Macromolecules* **2010**, *43*, 6024–6032
DOI: 10.1021/ma100847g

Macromolecules
ARTICLE

Synthesis and Properties of a Series of Mesogen-Jacketed Liquid Crystalline Polymers with Polysiloxane Backbones

Lanying Zhang, Si Chen, Han Zhao, Zhihao Shen,* Xiaofang Chen, Xinghe Fan,* and Qifeng Zhou*

Beijing National Laboratory for Molecular Sciences, Key Laboratory of Polymer Chemistry and Physics of Ministry of Education, College of Chemistry and Molecular Engineering, Peking University, Beijing 100871, China

Received April 17, 2010; Revised Manuscript Received June 8, 2010

ABSTRACT: A series of mesogen-jacketed liquid crystalline polymers (MJLCPs) with polysiloxane backbones have been synthesized by hydrosilylation of polymethylhydrosiloxane with styrenic derivatives. Their properties were studied in detail by a combination of ^{1}H NMR, Fourier transform infrared spectroscopy, differential scanning calorimetry, polarized light microscopy, wide-angle X-ray diffraction, scanning electron microscopy, and contact angle measurements. Wide-angle X-ray diffraction results indicated that these MJLCPs based on highly flexible polysiloxane main chain could also self-assemble into supramolecular columnar nematic or smectic liquid crystalline phases compared with structurally similar MJLCPs having a polyethylene backbone, but their liquid crystalline ranges were narrowed significantly. Low contact-angle values of the MJLCPs could be attributed to the fact that the polysiloxane backbones were embedded in mesogenic side chains, which also confirmed the mesogen-jacketed model for MJLCPs.

Introduction

Studies on the synthesis, properties, and applications of structurally abundant side-chain liquid crystalline polymers (SCLCPs) have attracted great interest over the past few decades[1] due to the fact that these polymers represent improved properties over low molecular weight liquid crystalline (LC) materials and have outstanding applications such as nonlinear optic devices, optical data storage materials, and so on.[2] In SCLCPs, siloxane polymers play a vital role on obtaining not only synthetic techniques but also thermal and mechanical stabilities. On the other hand, siloxane polymers are of considerable interest because their highly flexible Si−O bond provides materials that have much lower T_g than liquid crystalline polyacrylates and polymethacrylates and are useful in certain applications. Polysiloxane liquid crystalline polymers with specific structures can be obtained by hydrosilylation of polymethylhydrosiloxane with alkenes using Pt complexes as catalysts. Polysiloxane polymers with mesogenic units terminally or laterally attached to the polymers are widely researched for their structure−property relationships.

Finkelmann et al. first synthesized polysiloxane liquid crystalline polymers by hydrosilylation between hydrogen-containing silicone oil and vinyl liquid crystalline monomers[3,4] in 1979. During 1987−1991, Percec et al. reported a series of liquid crystalline polysiloxanes containing macroheterocyclic ligands,[5] half-disk and rodlike moieties,[6] heterocycloalkanediyl groups,[7,8] and methylstilbene groups.[9,10] The side-chain mesogenic units were all terminally attached to the poly(methylsiloxane)s and poly(methylsiloxane-*co*-dimethylsiloxane) through flexible spacers containing at least three methylene units, and these polymers showed two glass transitions, one of which was assigned to the independent motion of the polymer backbone and the other to the cooperative (but independent from that of the polymer backbone) motion of the side groups. The effect of the polymer backbone and the spacer length on the mesophase and crystallization was also investigated. Hardouin et al. investigated the influencing factors of the molecular parameters of side-chain liquid crystalline polysiloxanes and "diluted" copolysiloxanes on the mesomorphic, thermodynamic, and structural properties. They synthesized several series of side-chain liquid crystalline polysiloxanes or copolysiloxanes with the mesogenic groups laterally attached (the so-called side-on fixed) to the polymer main chain through at least 4 or more methylenic units and an ester group,[11−17] and found that the spacer length, the aliphatic tail length, and the content of mesogenic groups ("dilution" effect) all had great influences. Main-chain liquid crystalline polymers (MCLCPs) with mesogenic units and siloxane spacers in the main chain were also synthesized and studied,[18−20] and results revealed that the flexible spacers rendered the semiflexible polymers with low thermal transitions. Functional liquid crystalline polymers based on polysiloxane, such as polymers with high-efficiency blue-light emitting properties,[21] gas transport properties,[22] ferroelectric properties,[23] or those applicable in gas chromatography,[24] and polymers with special structures such as ladder-like,[25−27] fishbone-like[28] or linear and hyperbranched[29] polymers, were also synthesized and systematically investigated.

Mesogen-jacketed liquid crystalline polymers (MJLCPs), one special type of SCLCPs, were first proposed by Zhou et al. in late 1980s.[30,31] Different from Finkelmann's principle of obtaining traditional SCLCPs with flexible spacers to decouple interactions between the main chain and the mesogenic side groups and achieve liquid crystallinity,[32,33] MJLCPs were constructed by mesogens linking to the main chain at the waist or mass center position through only one covalent C−C bond or a very short spacer. The bulky and rigid mesogenic units which were directly linking to the polymer backbone force the main chain to take an extended chain conformation and the "jacket" is thus formed. So MJLCPs are a kind of rigid or semirigid polymers and exhibit properties similar to those of MCLCPs. This concept has been confirmed by experimental results using X-ray diffraction[34] and small-angle neutron scattering.[35−38]

*To whom correspondence should be addressed. E-mail: (X.F.) fanxh@pku.edu.cn; (Z.S.) zshen@pku.edu.cn; (Q.Z.) qfzhou@pku.edu.cn.

 Published on Web 06/28/2010

Scheme 1. Representative Chemical Structures of the Corresponding Conventional MJLCPs

Conventional MJLCPs	Chemical structure
PMPCS	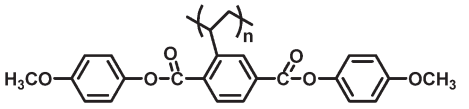
PBPCS	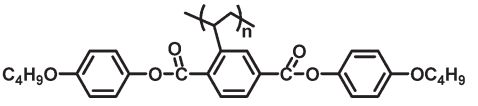
OXD-C12p	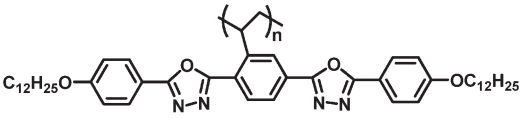
4C2Vp	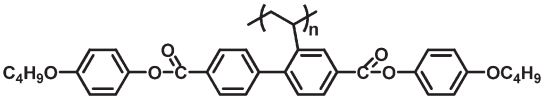
12C2Vp	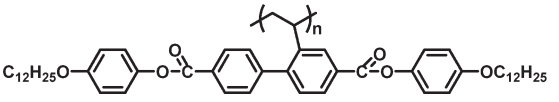

Since the first publication of MJLPCs, up to now, many kinds of MJLCPs based on hydroquinone,[30] 2-vinylhydroquinone,[31] 2-vinylterephthalic acid,[39−41] 2 (or 3)-vinylbiphenyl-4,4′-dicarboxylic acid[42,43] with functional groups and unique structures have been designed and successfully synthesized. From the liquid crystalline phase point of view, in all these polymers, columnar nematic phase (Φ_N) is the most common phase observed. Higher ordered LC phases, such as hexatic columnar nematic phase (Φ_{HN}), hexagonal columnar phase (Φ_H),[41,43] rectangular columnar phase (Φ_R),[44] and smectic phase (S_A or S_C),[41−43] have also been reported. Additionally, siloxane moieties such as silsesquioxane core or poly(dimethylsiloxane) (PDMS) were also introduced into the structures, thus organic−inorganic hybrid liquid crystals,[45] star MJLCPs,[46] rod−coil diblock,[47] and triblock copolymers[48] with unique properties were obtained.

In the present paper, we report the synthesis and characterization of several examples of MJLCPs with polysiloxane as the polymer main chain. The particular examples described here refer to poly{[bis(4-methoxyphenyl) 2-ethylterephthalate]siloxane} (Si-MPCS), poly{[bis(4-butoxyphenyl) 2-ethylterephthalate]siloxane} (Si-BPCS), poly{[5,5′-(2-ethyl-1,4-phenylene)bis(2-(4-(dodecyloxy)phenyl)-1,3,4-oxadiazole)]siloxane} (Si-OXD-C12p), poly{[bis-(4-butoxyphenyl) 2-ethylbiphenyl-4,4′-dicarboxylate]siloxane} (Si-4C2Vp), poly{[bis(4-(dodecyloxy)phenyl) 2-ethylbiphenyl-4,4′-dicarboxylate]siloxane} (Si-12C2Vp). Different from the work by Hardouin et al. on mesogen-jacketed polysiloxanes,[11−17] the polysiloxane polymers in this study had a spacer length of only two methylenic units which laterally connected different types of mesogens to the polysiloxane backbone. Compared with the corresponding conventional MJLCPs with polyethylene backbone (see Scheme 1), this new series of MJLCPs based on polysiloxane backbone could still self-organize into columnar or smectic phase structures on the basis of WAXD analysis. On the other hand, we anticipate that introduction of the flexible polysiloxane backbone may offer the polymers more interesting properties and potential applications.

Experimental Section

Materials. Polymethylhydrosiloxane (PHMS, M_n = 1 700−3 200 g/mol, Aldrich Chemical Co., Inc.) and platinum(0)-1,3-divinyl-1,1,3,3-tetramethyldisiloxane complex (Pt(dvs), in xylenes (∼2% Pt), Aldrich) were used as received. Tetrahydrofuran (THF) was distilled from Na/benzophenone under Ar for at least 8 h until the solution turned blue.

Equipment and Measurements. ^{1}H NMR (400 MHz) spectra were recorded on a Bruker ARX400 spectrometer using deuterated chloroform ($CDCl_3$) with tetramethylsilane as the internal standard at room temperature for styrenic derivatives and deuterated chloroform ($CDCl_3$) without tetramethylsilane at room temperature for the polymers.

Fourier transform infrared spectroscopy (FTIR) was conducted on a Nicolet Magna-IR 750 Fourier transform infrared spectrometer with the method of infrared microscopy.

Thermogravimetric analysis (TGA) was performed on a TA SDT 2960 instrument at a heating rate of 20 °C/min in a nitrogen atmosphere.

Differential scanning calorimetry (DSC) examination was carried out on a TA DSC Q100 calorimeter with a programmed heating procedure under nitrogen. The sample size was about 5 mg and encapsulated in hermetically sealed aluminum pans, whose weights were kept constant. The temperature and heat flow scale at different cooling and heating rates were calibrated using standard materials such as indium and benzoic acid.

Polarized light microscopy (PLM) observation of the liquid crystalline textures of the polymers was performed on a Leitz Laborlux 12 microscope with a Leitz 350 hot stage. The image was captured using an insight digital camera. The film was prepared by solution-casting from THF. The specimens were slightly sheared to increase the LC domain size.

One-dimensional (1D) wide-angle X-ray diffraction (WAXD) experiments were performed on a Philips X'Pert Pro diffractometer with a 3 kW ceramic tube as the X-ray source (Cu Kα) and an X'celerator detector. The reflection peak positions were calibrated with silicon powder ($2\theta > 15°$) and silver behenate ($2\theta < 10°$). In a typical experiment, a sample of about 40 mg was cast from a THF solution. The sample stage was set horizontally, and a temperature control unit (Paar Physica TCU 100) in conjunction with the diffractometer was utilized to study the structure evolution as a function of temperature. The heating and cooling rates in the WAXD experiments were 5 °C/min.

Two-dimensional (2D) WAXD patterns were obtained using a Bruker D8Discover diffractometer with GADDS as the 2D detector. Silicon powder and silver behenate were used as standards. The 2D diffraction patterns were recorded in a

Scheme 2. Synthesis and Structures of the Mesogen-Jacketed Polysiloxanes

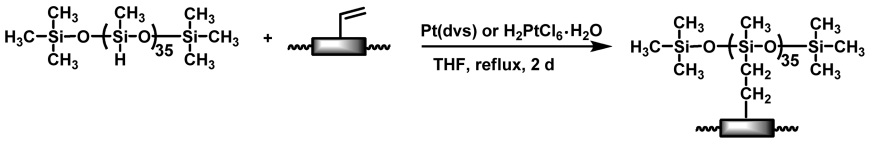

Mesogen-jacketed polysiloxanes	
Si-MPCS	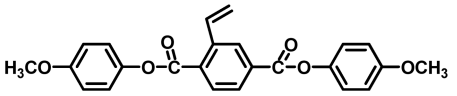
Si-BPCS	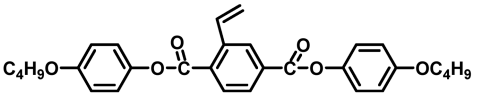
Si-OXD-C12p	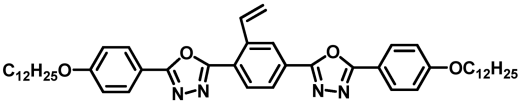
Si-4C2Vp	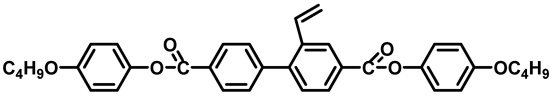
Si-12C2Vp	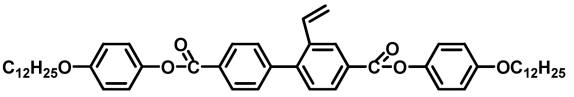

transmission mode at room temperature. The oriented samples were prepared by mechanically shearing the films at the temperatures in their liquid crystalline phase. The sample was mounted on the sample stage and the point-focused X-ray beam was aligned either perpendicular or parallel to the mechanical shearing direction.

Scanning electron microscopy (SEM) measurements of the dry samples spin-coated on glass slides were carried out on a model S-4800 field emission electron microscope to identify the surface morphology of selected polymers.

Contact angle (CA) measurements were conducted using an optical contact angle meter system (Dataphysics Inc., OCA20, Germany). The polymer sample of 10 mg was dissolved in THF at a concentration of 10 mg/mL. The resulting solution was then spin-coated on a clean glass slide to allow the solvent to evaporate, after which the sample was dried for 5 h in an oven at room temperature. The measurements of each sample were repeated three times in order to minimize statistical variations.

Synthetic Procedure. *Synthesis of the Styrene Derivatives.* All the styrene derivatives were synthesized according to the procedures reported by our lab previously.[39−42]

Synthesis of the Corresponding Polymers with Polysiloxane Backbone. These polymers were synthesized by hydrosilylation of polymethylhydrosiloxane with the styrene derivatives using Pt(dvs) as the catalyst. A typical procedure was as follows using the synthesis of Si−MPCS as an example:

2,5-Bis[(4-methoxyphenyl)oxycarbonyl]styrene (MPCS) (0.501 g, 1.240 mmol) and polymethylhydrosiloxane (0.067 g, 0.021 mmol) were dissolved in 60 mL of dry, freshly distilled THF under Ar atmosphere. Pt(dvs) dissolved in xylenes (5 μL) was added to the stirred solution, then the system was heated at reflux under anhydrous conditions for 2 d. The mixture was then cooled to room temperature, filtered, concentrated, and poured into 300 mL methanol. The mixture was stirred and filtered off. The solid was collected and dissolved in chloroform, then precipitated in methanol (three times), and dried at 40 °C under vacuum for 24 h.

Results and Discussion

Synthesis and Characterization of the Polymers. The synthesis and structures of the polymers are shown in Scheme 2. Target polymers were synthesized by the hydrosilylation of polymethylhydrosiloxane with the styrene derivatives using Pt(dvs) as the catalyst. The chemical structures of all the polymers were confirmed by FTIR and ^{1}H NMR spectroscopic methods.

With Si-MPCS as an example, FTIR spectra of Si-MPCS and PHMS and ^{1}H NMR spectra of MPCS and Si-MPCS are presented in Supporting Information. The disappearance of the sharp vibrational band at 2170 cm^{-1} assigned as the Si−H stretching showed that all the Si−H groups were reacted completely. The appearance of the vibrational bands at 2840−2960, 1700, 1470−1600, and 1260−1040 cm^{-1} which were attributed to vibrations from aliphatic chain (C−H), ester carbonyl (C=O), aromatic (Ar), and Si−O, respectively, illustrated the successful preparation of the polymer. From the ^{1}H NMR spectra, the chemical shifts at δ = 4.7 ppm attributed to Si−H proton and δ = 5.34 and 5.44 ppm attributed to ethylene proton disappeared in the polymers, indicating complete reaction of the Si−H groups. The ^{1}H NMR spectrum of the resulting polysiloxane Si-MPCS showed broad peaks instead of sharp ones, typical for polymers

Table 1. Molecular Weights and Thermal Properties of the Polymers

polymer	M_n (g/mol)[a]	T_g (°C)[b]	T_d (°C)[c]
Si-MPCS	16 600	111 (118)	344
Si-BPCS	19 500	92 (98)	368
Si-OXD-C12p	29 200	156 (167)	310
Si-4C2Vp	22 200	96 (105)	383
Si-12C2Vp	30 000	76 (86)	407

[a] Calculated according to a polymerization degree of 35. [b] Evaluated by DSC at a rate of 10 °C/min. The data in the parentheses denote the T_g values of the corresponding styrenic polymers. [c] The temperature at which 5% weight loss of the sample from TGA-DSC under nitrogen atmosphere at a heating rate of 10 °C/min.

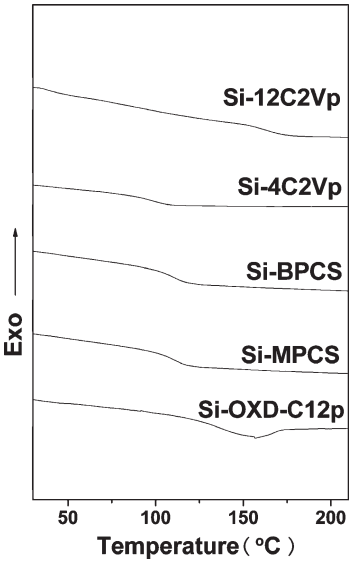

Figure 1. Differential scanning calorimetry thermograms of the five polysiloxane polymers during second heating at a scanning rate of 10 °C/min.

due to the slower motion of the protons. It is worthy of noting that the single peak assigned to OCH_2 at $\delta = 3.7$ ppm split into doublets in the polymers, which was very similar to the case of the corresponding MJLCPs with polyethylene backbone, poly{2,5-bis[(4-methoxyphenyl)oxycarbonyl]-styrenes} (PMPCS).

Phase Transitions and Phase Structures of the Polymers. The phase behaviors of all the polymers were investigated by DSC, PLM, and WAXD. The thermal properties of this new class of mesogen-jacketed polymers are listed in Table 1.

The M_n values of all the mesogen-jacketed polysiloxanes were calculated according to the polymerization degree of the polysiloxane. As shown in Table 1, the temperatures at 5% weight loss under N_2 (T_d's) were all over 310 °C, indicating that all the polymers had good thermal stabilities. In order to avoid thermal degradation, all the characterizations were carried out at temperatures well below T_d. The DSC experiments of all the polymers showed apparent glass transitions during the first cooling and subsequent heating scans (Figure 1) and no other phase transitions were observed except for Si-BPCS (Figure 2). Comparing the glass transition temperatures (T_g's) of the polysiloxane polymers in this study with those of the corresponding conventional MJLCPs, we found that T_g's of the polysiloxanes were about 10 °C lower, which might be contributed to combined effect of the flexible polysiloxane backbone and the less rigid side-chain structure with the introduction of the ethylene spacer. Figure 2 presents DSC thermograms of polymer Si-BPCS during the first cooling and second heating cycles at a rate of 10 °C/min. Besides the glass transition, a small first-order

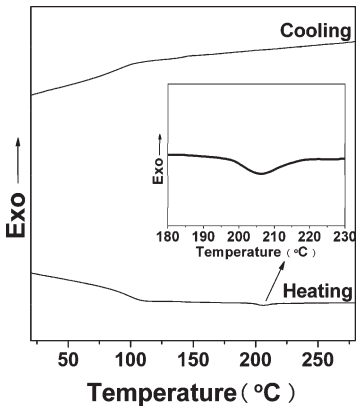

Figure 2. Differential scanning calorimetry thermograms of Si-BPCS during the first cooling and second heating at a scanning rate of 10 °C/min. The inset is the enlarged part during heating between 180−230 °C.

transition process was observed at about 230 °C (as shown in the inset) during the heating cycle and the heat of transition of the endothermic process was very small. Compared with poly{2,5-bis[(4-butoxyphenyl)oxycarbonyl]styrenes} (PBPCS) having a comparable molecular weight, the behavior of Si-BPCS was very similar.

To investigate the LC phase behaviors of all the polymers, PLM, 1D WAXD, and 2D WAXD experiments were conducted.

Si-MPCS. The phase transition of an as-cast Si-MPCS sample was evidenced by 1D WAXD patterns at different temperatures. Sets of 1D WAXD profiles recorded during the first heating and subsequent cooling are presented in Figure 3. The isotropic sample rendered two amorphous halos in low- and high-angle regions, respectively, at room temperature. At 240 °C, a shoulder appeared at the high-angle side of the low-angle halo (the dashed curves in Figure 3b are the deconvoluted halo and peak) and developed into a reflection peak with a further increase in temperature. This reflection peak had a 2θ value of 5.5° with a d-spacing of 1.59 nm at 250 °C, which was about the same as that of PMPCS with M_n in the range of 1.0×10^4 and 1.6×10^4 g/mol. During the subsequent cooling, the reflection peak and scattering halo were retained down to room temperature. The intensities of both the reflection peak and the scattering halo decreased with decreasing temperature. This result indicated that similar to PMPCS, Si-MPCS developed an LC phase during heating, and the LC phase remained during cooling.

Since the 1D WAXD patterns lack dimensionality, we employed 2D WAXD to identify the phase structure. The sample was oriented at 210 °C during cooling from higher temperatures and annealed for several hours. Parts a and b of Figure 4 show two 2D WAXD patterns at room temperature of the oriented, annealed sample, with the X-ray incident beam perpendicular (along the Y direction) and parallel to the shear direction (along the X direction), respectively. In Figure 4a, when the shear direction was parallel to the meridian direction, a pair of strong diffraction arcs could be observed on the equator, indicating the development of ordered structures on the nanometer scale with lattice planes oriented primarily parallel to the meridian. In addition, scattering halos in the high-angle region were more or less concentrated on the meridian with rather broad azimuthal distributions, which revealed that subnanometer structures with short-range order existed mainly along the meridian direction. On the other hand, A ring pattern is shown in Figure 4b, which exhibited an isotropic intensity distribution in the azimuthal scan. Therefore, the LC phase of Si-MPCS should be a Φ_N

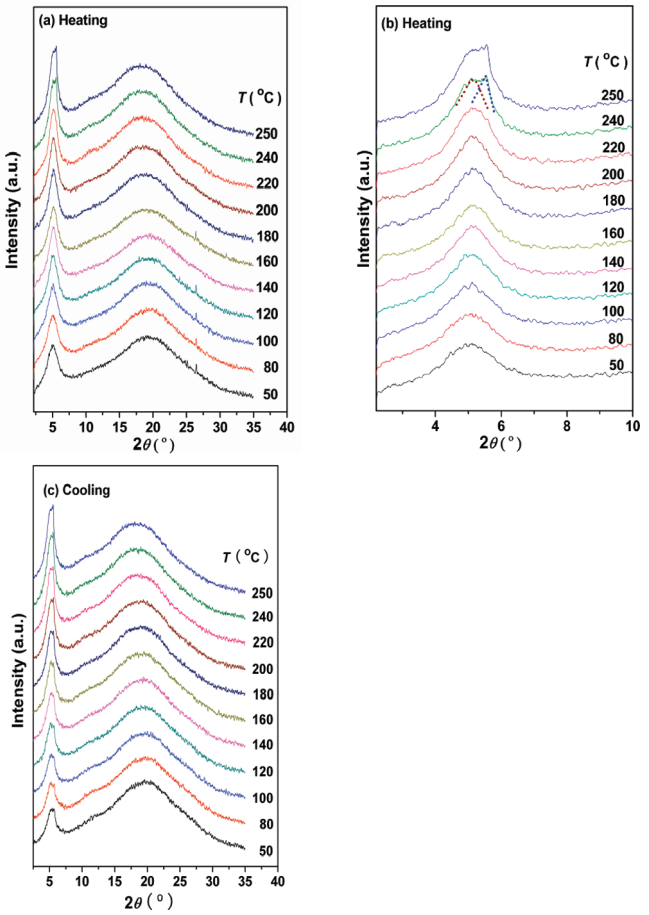

Figure 3. Sets of 1D WAXD patterns of sample Si-MPCS recorded upon heating (a) (part b shows the enlarged patterns in the low-angle region during heating) and subsequent cooling (c) at various temperatures.

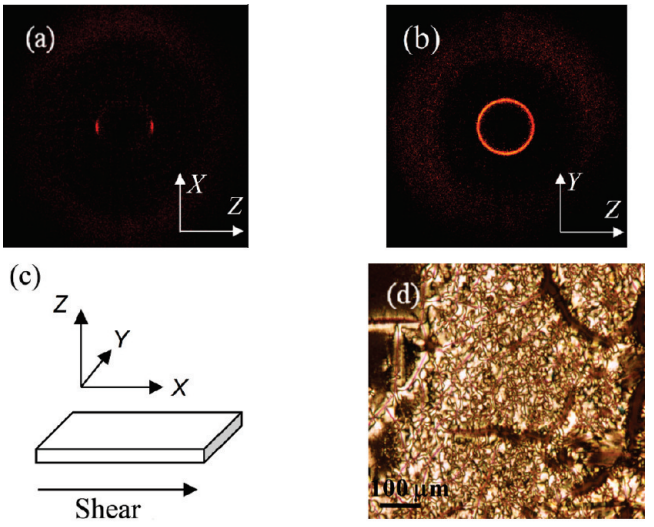

Figure 4. Two-dimensional wide-angle X-ray diffraction patterns of sheared sample Si-MPCS recorded at room temperature with the X-ray incident beam along the *Y* direction (a) or the *X* direction (b); schematics of shearing geometry (c); polarized light microscope image of the sample at 230 °C (d).

phase.[49] The Φ_N phase assignment was further supported by the PLM observations. The as-cast film showed very weak birefringence at low temperatures. However, birefringent textures appeared during the first heating after the samples

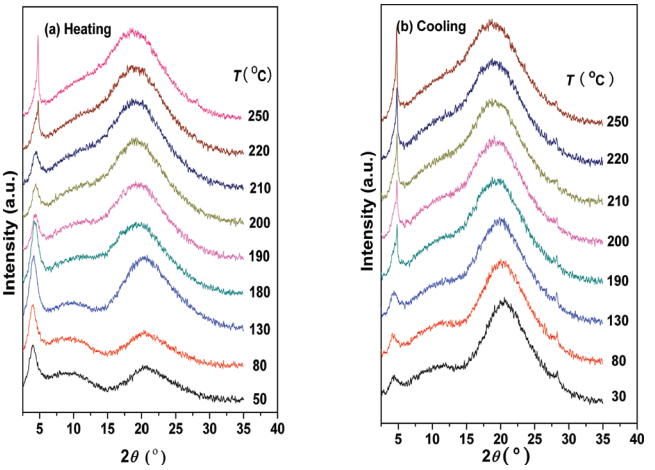

Figure 5. Sets of 1D WAXD patterns of sample Si-BPCS recorded upon heating (a) and subsequent cooling (b) at various temperatures.

reached the temperatures at which the reflection peaks started to develop in the 1D WAXD experiments. The texture evidenced in Figure 4d was similar to that of PMPCS with M_n in the range of 1.0×10^4 and 1.6×10^4 g/mol, in which PMPCS had a Φ_N phase, implying a columnar nematic LC structure. The LC texture of the sample remained unchanged during cooling, which was also similar to the behavior of PMPCS.

Si-BPCS. To confirm the phase transition of Si-BPCS which was indicated by DSC investigation, 1D WAXD was first conducted. Sets of 1D WAXD patterns of the as-cast Si-BPCS sample obtained during the first heating and the first cooling are illustrated in Figure 5, parts a and b. The isotropic sample rendered an amorphous halo in the low-angle region at low temperatures. After 180 °C, the intensity of the halos decreased significantly, while at temperatures above 220 °C, a sharp and intense peak appeared at a higher 2θ value of 4.75° (with a *d*-spacing of 1.86 nm). This peak became weak and disappeared below 190 °C on the subsequent cooling scan. The distinct discontinuous change in intensity corresponded to the endothermic transition at about 210° shown in the DSC thermogram during the second heating scan. This observation during cooling clearly suggested that the LC phase was formed at higher temperature. The similar unusual behavior was also observed in our previous studies with the sample PBPCS.[40] As is common for MJLCPs, the phase behavior of PBPCS is molecular weight-dependent. The molecular weight of Si-BPCS is close to the lower limit of that for PBPCS to be able to develop into the liquid crystalline phase. Moreover, due to the brittleness and the disappearance of the LC phase at room temperature for Si-BPCS, it was difficult to conduct 2D WAXD experiments on the sample, and no obvious birefringence changes were observed in PLM observation. But from the results obtained from DSC and 1D WAXD experiments, including the *d*-spacing values for Si-BPCS and PBPCS, we temporarily assigned the LC phase of Si-BPCS as a Φ_{HN} phase, similar to that of PBPCS.

Si-OXD-C12p. To elucidate the phase structure and transition of Si-OXD-C12p, we performed WAXD and PLM experiments. Sets of 1D WAXD patterns of the Si-OXD-C12p sample obtained during the first heating and the subsequent cooling are shown in Figure 6, parts a and b, respectively. The sample prepared by solution-casting from a THF solution was amorphous due to the fast solvent evaporation that froze the chain motion. Upon the first heating in Figure 6a, a diffraction peak rapidly developed and the peak slightly shifted to a lower angle, indicating the

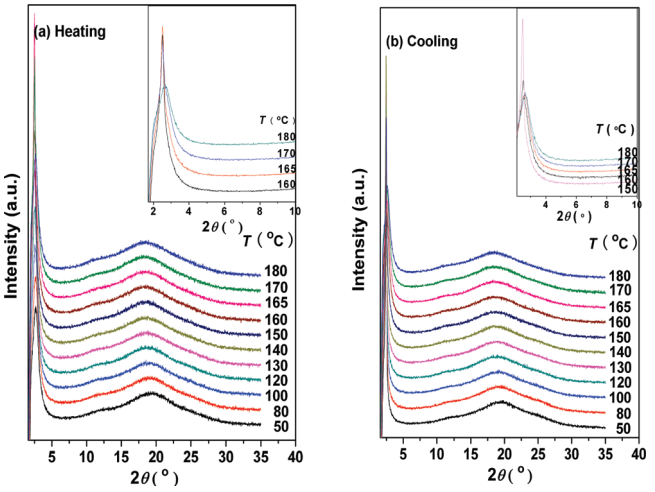

Figure 6. Sets of 1D WAXD patterns of sample Si-OXD-C12p recorded upon heating (inset shows the enlarged patterns in the low-angle region) (a) and subsequent cooling (inset shows the enlarged patterns in the low-angle region) (b) at various temperatures.

development of an ordered phase, possibly an LC phase. When the temperature exceeded 170 °C, the diffraction peak disappeared and became a scattering halo (see the inset of Figure 6a), indicating that the sample became isotropic. On the other hand, the diffraction could be restored at 160 °C and retained below the T_g of the sample upon cooling as can be seen in Figure 6b. In order to elucidate whether higher-order diffractions were present, we also tried more sample amounts and longer exposure times as what have been done for corresponding conventional MJLCPs, poly{2,5-bis[(4-alkoxy-phenyl)-1,3,4-oxadiazole]styrene} (OXD-C12p). However, unfortunately, no higher-order diffraction was observed.

A 2D WAXD experiment was employed to obtain the dimensional information. A sample was mechanically sheared and annealed at 145 °C after cooled from the isotropic state. Figure 7a shows the 2D WAXD pattern of the oriented Si-OXD-C12p sample recorded at room temperature with the X-ray incident beam perpendicular (along Y direction) to the shear direction (X direction). In this figure, when the shear direction was parallel to the meridian direction, a very strong diffraction pair with a d-spacing of 3.53 nm could be observed on the equator, and four scattering halos in the high-angle region appeared in the quadrants with rather broad azimuthal distributions. The corresponding azimuthal intensity profile shown in Figure 7b exhibited four maxima with an angle of about 80° between the two adjacent diffraction maxima in the range of 50−150°, although the intensities were not exactly identical, which might be caused by an imperfection in the sample alignment during the experiment. A similar pattern was obtained when the X-ray incident beam was parallel to the shear direction, as exhibited in Figure 7c. The similarity of these two patterns indicated that the sample might be in a smectic phase. Combined with the result shown in Figure 7b, the LC phase could be determined to be an S_C phase with a tilt angle of approximately 40° (80°/2). The PLM micrograph in Figure 7d confirmed the existence of an LC phase.

Si-4C2Vp. The phase behavior of the sample Si-4C2Vp was verified by 1D WAXD experiments. Parts a and b of Figure 8 shows the structurally sensitive 1D WAXD patterns of the sample from 50 to 250 °C. The as-cast amorphous sample demonstrated two scattering halos in a low-angle region of 2−5° and a high-angle region of 15−25° at low temperatures. Upon the first heating below T_g (Figure 8a), the scattering halos slightly shifted to lower angles due to thermal expansion and

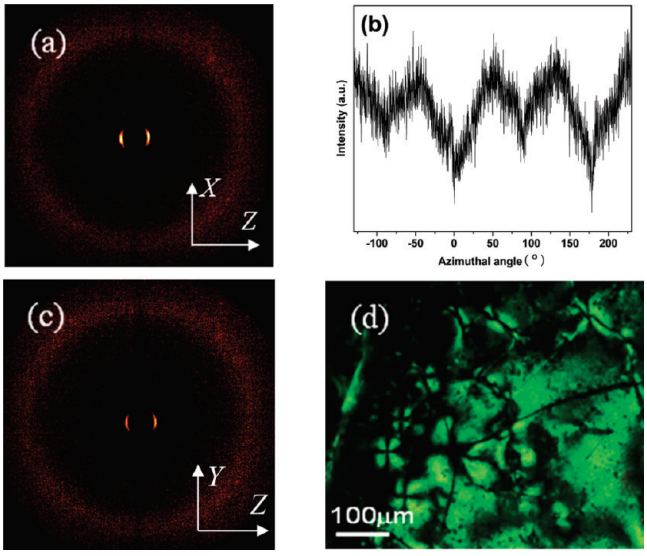

Figure 7. Two-dimensional wide-angle X-ray diffraction patterns of a sheared Si-OXD-C12p sample recorded at room temperature with the X-ray incident beam along the Y direction (a) (part b shows the azimuthal scanning data of the high-angle diffraction in part a) or the X direction (c); polarized light microscope image of the sample at 145 °C (d).

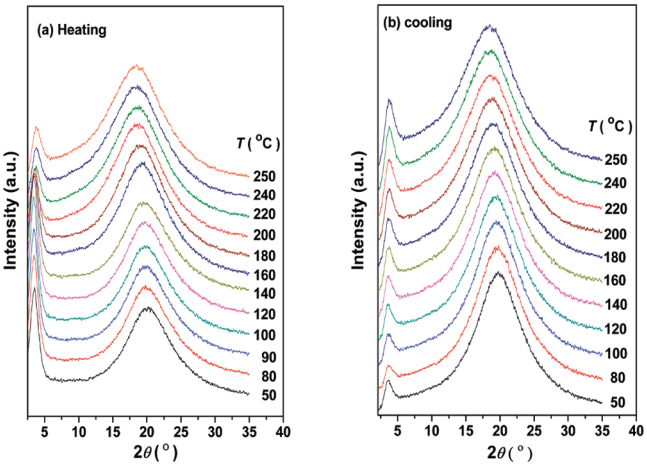

Figure 8. Sets of 1D WAXD patterns of sample Si-4C2Vp recorded upon heating (a) and subsequent cooling (b) at various temperatures.

their intensities increased slightly. Further heating led to a rapid decrease in the intensity of the low-angle halo. The intensity of the halo continued decreasing upon cooling while the high-angle halo which reflected liquid-like short-range order on the subnanometer scale became relatively strong (Figure 8b), indicating that this polymer was amorphous during the whole temperature range. No birefringent textures were observed in PLM experiments throughout the whole temperature range, which confirmed that Si-4C2Vp was amorphous.

Si-12C2Vp. The phase transition of Si-12C2Vp was verified by 1D WAXD experiment at various temperatures. Parts a and b of Figure 9 present the changes of the structurally sensitive 1D WAXD patterns of Si-12C2Vp during heating and subsequent cooling. Upon the first heating (Figure 9a), a diffraction peak at a low 2θ value of 2.08° (d = 4.24 nm), indicating the existence of an ordered phase, possibly an LC phase, and a scattering halo in the wide-angle region were observed from the WAXD patterns of the as-cast amorphous sample. No higher-order diffractions could be observed in the 1D WAXD experiment. When the temperature

exceeded 180 °C, a diffuse halo appeared in the vicinity of the sharp peak in the low-angle region (as shown in the inset of Figure 9a), and the intensity of this halo increased with increasing temperature until the sharp peak disappeared completely at 240 °C, indicating that the sample entered into the isotropic state. Upon cooling (Figure 9b), the sharp peak which originated from the LC phase developed again, and the diffraction peak and the scattering halo could be preserved down to room temperature.

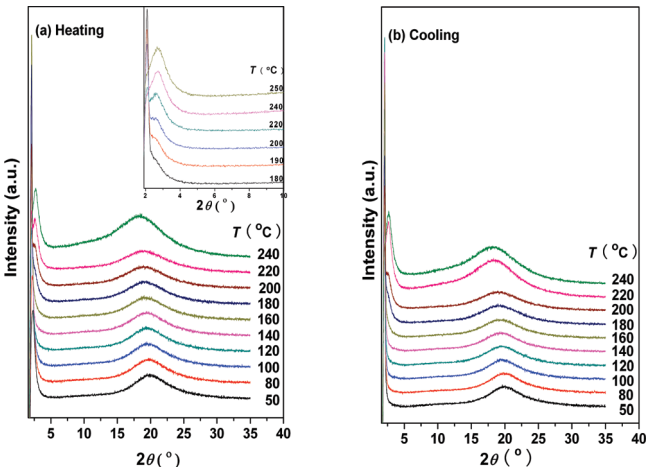

Figure 9. Sets of 1D WAXD patterns of sample Si-12C2Vp recorded upon heating (inset shows the enlarged patterns of the sample in the low-angle region) (a) and subsequent cooling (b) at various temperatures.

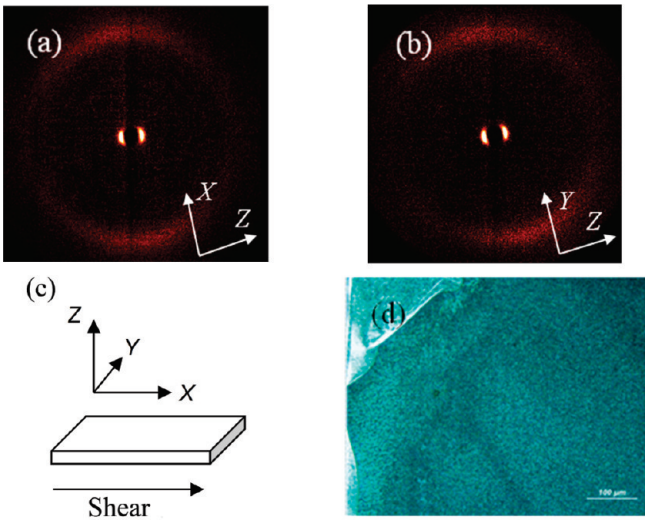

Figure 10. Two-dimensional wide-angle X-ray diffraction patterns of a sheared Si-12C2Vp sample recorded at room temperature with the X-ray incident beam along *Y* direction (a) or *X* direction (b); schematics of shearing geometry (c); polarized light microscope image of the sample at 130 °C (d).

To further identify the phase structure of the LC phase, a 2D WAXD experiment was carried out. A film sample of Si-12C2Vp was mechanically sheared at 165 °C and annealed for several hours. Figures 10a and 10b show the 2D WAXD patterns with the X-ray incident beam perpendicular (along the *Y* direction) and parallel to the shear direction (along the *X* direction). In Figure 10a, a pair of strong diffraction arcs could be found on the equator at $2\theta = 2.09°$, indicating the presence of an ordered structure on the nanometer scale. Meanwhile, a pair of scattering halos in the high-angle regions which represented short-range order was more or less concentrated on the meridian with rather broad azimuthal distributions. This 2D WAXD pattern suggested that the sample was probably in a columnar nematic or an S_A phase. On the other hand, when the incident beam was along *X* direction (Figure 10b), the 2D WAXD pattern was very similar to that shown in Figure 10a, indicating that the Si-12C2Vp sample developed an S_A phase. Furthermore, the birefringent texture shown in Figure 10d obtained from PLM experiment during heating was similar to the sand-like texture in literature,[50] also evidencing the existence of an LC phase. The birefringence disappeared when the sample was heated to above 180 °C, which was consistent with the 1D WAXD results.

Dependence of Mesophase Behavior on Polymer Molecular Structure. Since the concept of MJLCPs was first proposed by Zhou and co-workers, many kinds of MJLCPs with various structures and properties have been designed and successfully synthesized. Moreover, dependence of the phase structure on the chemical structure of the polymer repeating unit has also been investigated. Studies have shown that the phase structures of MJLCPs can be tuned by a few factors, such as the molecular weight,[39,40] the terminal alkyl length,[39,40,43] the shape of the mesogens,[44] molecular architecture,[46] and so on. But from the present work, we can conclude that by changing the polymer backbone and moderately increasing the length of the spacer, their LC phase can also be different compared with conventional MJLCPs. As shown in Table 2, the *d*-spacing values of the polysiloxane polymers were all close to those of the corresponding MJLCPs based on polyethylene backbone. The phase structures of the polysiloxanes might be similar to or largely different from their counterparts with polyethylene backbones. For example, Si-MPCS and PMPCS both showed columnar nematic phases. On the other hand, while 4C2Vp, the conventional MJLCP, exhibited an S_A phase, Si-4C2Vp did not show liquid crystalline behavior when the polymer backbone was changed to polysiloxane. The dependence of the phase structure on the number of aromatic rings in the mesogens of the polysiloxanes in this study was schematically presented in Figure 11, although the phase structures of MJLCPs depend not only on the length of the rigid core, but also on the length of the flexible tails, the substitution positions on the rigid core, and other factors. For the LC polysiloxanes in the present work, we found again that the polymers tend to form smectic phases when increasing the rigidity of the mesogens of MJLCPs.

Hydrophilic/Hydrophobic Properties of the Polymers. It is well-known that PDMS has low surface energy and exhibits high hydrophobic property. We also measured the

Table 2. Comparison of LC Phases between Mesogen-Jacketed Polysiloxane and Conventional MJLCPs with Polyethylene Backbones

mesogen-jacketed polysiloxanes	LC phase	*d*-spacing (nm)	conventional MJLCPs	LC phase	*d*-spacing (nm)
Si-MPCS	Φ_N	1.58	PMPCS	Φ_N[a]	1.59
Si-BPCS	Φ_{HN}	1.86	PBPCS	Φ_{HN}	1.87
Si-OXD-C12p	S_C	3.53	OXD-C12p	S_A	3.44
Si-4C2Vp	No		4C2Vp	S_A	3.00
Si-12C2Vp	S_A	4.24	12C2Vp	S_C	4.20

[a] For the polymers with M_n in the range of 1.0×10^4 and 1.6×10^4 g/mol.

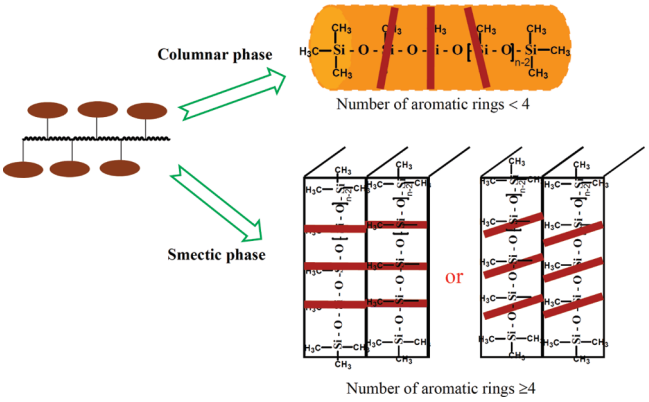

Figure 11. Dependence of phase structure on the number of aromatic rings in the mesogens of the mesogen-jacketed polysiloxanes obtained in this study.

water CA values of the polymers synthesized in this study at room temperature. It has been reported that the wetting behavior of a solid surface is governed by two factors, surface roughness and chemical composition. Increasing surface roughness and lowering surface tension can dramatically enhance surface water repellency.[51] To avoid the effect of surface roughness, the samples of 10 mg were dissolved in THF at a concentration of 10 mg/mL. The resulting solutions were then spin-coated on clean glass slides to allow the solvent to evaporate under the same conditions, and dried for 5 h under vacuum. The resultant coatings exhibited no obvious microstructures by SEM investigation (see Supporting Information Figure S3). Water CA values of the surfaces were only 83.3 ± 1.2° and 91.4 ± 1.6° for the samples Si-MPCS and Si-BPCS, respectively (the insets of each Figure S3a,b), only a little higher compared with those of the corresponding conventional MJLCPs, PMPCS and PBPCS (the insets of each Figure S3c,d). While the water CA value of polystyrene (PS) cast from a 5 mg/mL solution in *N*,*N*-dimethylformamide (DMF) in dry air was 81.1 ± 1.5°,[52] and the typical surface water CA value of native PDMS was approximately 110°.[53] The hydrophobic/hydrophilic properties of the mesogen-jacketed polysiloxanes in this study were very similar to that of the conventional MJLCPs and PS. In other words, the introduction of the polysiloxane main chain did not significantly enhance the superhydrophobic property. As proposed in our previous studies on MJLCPs, the polysiloxane backbone was embedded in the side chains due to the "jacketing" effect of the laterally attached, bulky mesogens. Therefore, the polysiloxane main chain did not show its intrinsic superhydrophobicity, which also confirmed the mesogen-jacketed model. It is worth pointing out that with the increasing length of terminal alkyl tails in the mesogen, the CA value was somewhat increased, which was consistent with the hydrophobic nature of alkyl chains.

Conclusion

In summary, a series of new MJLCPs based on polysiloxane main chain were successfully synthesized and characterized. For the polysiloxane system with the mesogens laterally linking to the backbone, we reduced the spacer that connected the backbone and mesogens to only two methylene units. The chemical structures of all the polymers were confirmed by various characterization techniques. When 1D and 2D WAXD results were combined with PLM and DSC observations, their phase structures and transitions were investigated and confirmed. Compared with the corresponding conventional MJLCPs with polyethylene backbone, the introduction of highly flexible polysiloxane backbone generated a novel series of MJLCPs. They could still self-organize into supramolecular columnar nematic or smectic liquid crystalline phases with the polysiloxane backbones embedded in the mesogenic side chains on the basis of WAXD and CA analyses, but the LC temperature ranges were all decreased significantly. Furthermore, the CA results also confirmed the mesogen-jacketed model. We expect that these MJLCPs with the polysiloxane backbone will possess interesting properties and have potential applications.

Acknowledgment. Financial support from the National Natural Science Foundation of China (Grant Nos.: 20634010, 20874002, 20874003 and 20974002) is gratefully acknowledged.

Supporting Information Available: Tables and figures giving characterization results of FT-IR and ^{1}H NMR of the polymers and the SEM images of some polymers. This material is available free of charge via the Internet at http://pubs.acs.org.

References and Notes

(1) Dubois, J. C., LeBarny, P., Mauzac, M., Noel, C., Demus, D., Goodby, J. W., Gray, G. W., Spiess, H. W., Vill, V., Eds. *Handbook of Liquid Crystals*: VCH: Weinheim, Germany, 1998; Vol. *3*, p 207.
(2) Blumstein, A. *Polymeric Liquid Crystals*; Plenum Press: New York, 1985.
(3) Finkelmann, H.; Rehage, G. *Makromol. Chem. Rapid. Commun.* **1980**, *1*, 733–740.
(4) Finkelmann, H. *Macromol. Chem.* **1982**, *183*, 1245–1256.
(5) Percec, V.; Rodenhouse, R. *Macromolecules* **1989**, *22*, 4408–4412.
(6) Percec, V.; Heck, J. *Macromolecules* **1991**, *24*, 4957–4962.
(7) Percec, V.; Hahn, B. *Macromolecules* **1989**, *22*, 1588–1599.
(8) Percec, V.; Hahn, B.; Ebert, M.; Wendorff, J. H. *Macromolecules* **1990**, *23*, 2092–2095.
(9) Percec, V.; Tomazos, D. *Macromolecules* **1989**, *22*, 2062–2069.
(10) Percec, V.; Tomazos, D. *Macromolecules* **1989**, *22*, 1512–1514.
(11) Achard, M. F.; Leroux, N.; Hardouin, F. *Liq. Cryst.* **1991**, *10*, 507–517.
(12) Hardouin, F.; Mery, S.; Achard, M. F.; Mauzac, M. *Liq. Cryst.* **1990**, *8*, 565–575.
(13) Lecommandoux, S.; Achard, M. F.; Hardouin, F. *Liq. Cryst.* **1998**, *25*, 85–94.
(14) Lerouxt, N.; Mauzact, M.; Noirezs, L.; Hardouin, F. *Liq. Cryst.* **1994**, *16*, 421–428.
(15) Achard, M. F.; Lecommandoux, S.; Hardouin, F. *Liq. Cryst.* **1995**, *19*, 581–587.
(16) Hardouin, F.; Lecommandoux, S.; Achard, M. F. *Kor. Polym. J.* **1998**, *25*, 85–94.
(17) Lecommandoux, S.; Noirez, L.; Achard, M. F.; Hardouin, F. *Macromolecules* **2000**, *33*, 67–72.
(18) Frank, B.; Lutz, W.; Michael, H.; Robert, K. *Makromol. Chem.* **1990**, *191*, 1775–1785.
(19) Guerino, S.; Cristopher, K. O.; Terry, B.; Mario, P.; Lupu, A. *J. Polym. Sci., Polym. Chem.* **1995**, *33*, 1913–1916.
(20) Harshad, P. P.; Jian, L.; Ronald, C. H. *Macromolecules* **2007**, *40*, 6206–6216.
(21) Zhou, Q. L.; Zhang, J. T.; Ren, Z. J.; Yan, S. K.; Xie, P.; Zhang, R. B. *Macromol. Rapid Commun.* **2008**, *29*, 1259–1263.
(22) Kawakami, H.; Mori, Y.; Abe, H.; Nagaoka, S. *J. Membr. Sci.* **1997**, *133*, 245–253.
(23) Shenouda, I. G.; Chien, L. C. *Macromolecules* **1993**, *26*, 5020–5023.
(24) Ganicz, T.; Andrzej Stanczyk, W.; Chmielecka, J.; Kowalski, J. *Polym. Int.* **2009**, *58*, 248–254.
(25) Cao, X. Y.; Wang, L. T.; Li, B.; Zhang, R. B. *Polym. Adv. Technol.* **1997**, *8*, 657–661.
(26) Pramoda1, K. P.; Lin, Y. H.; Chen, W. Y.; Chung, T. S. *Polym. Bull.* **2001**, *47*, 55–63.
(27) Suna, J.; Tanga, H. D.; Jianga, J. Q.; Xiea, P.; Zhanga, R. B.; Fub, P. F.; Wu, Q. *Polymer* **2003**, *44*, 2867–2874.
(28) Xie, P.; Wan, Y. Z.; Zhou, B.; Hou, J. N.; Dai, D. R.; Li, Z.; Liu, D. S.; Zhang, R. B. *Macromol. Chem. Phys.* **1996**, *191*, 745–752.
(29) Ganicz, T.; Pakula, T.; Fortuniak, W.; Białecka-Florjańczyk, E. *Polymer* **2005**, *46*, 11380–11388.
(30) Zhou, Q. F.; Li, H. M.; Feng, X. D. *Macromolecules* **1987**, *20*, 233–234.

(31) Zhou, Q. F.; Zhu, X. L.; Wen, Z. Q. *Macromolecules* **1989**, *22*, 491–493.
(32) Finkelmann, H.; Happ, M.; Portugall, M.; Ringsdorf, H. *Macromol. Chem.* **1978**, *179*, 2541–2544.
(33) Hessel, F.; Finkelmann, H. *Polym. Bull.* **1985**, *14*, 375–378.
(34) Gray, G. W.; Hill, J. S.; Lacey, D. *Mol. Cryst. Liq. Cryst.* **1991**, *197*, 43–55.
(35) Hardouin, F.; Leroux, N.; Mery, S.; Noirez, L. *J. Phys. II* **1992**, *2*, 271–278.
(36) Leroux, N.; Keller, P.; Achard, M. F.; Noirez, L.; Hardouin, F. *J. Phys. II* **1993**, *3*, 1289–1296.
(37) Lecommandoux, S.; Achard, M. F.; Hardouin, F.; Brulet, A.; Cotton, J. P. *Liq. Cryst.* **1997**, *22*, 549–555.
(38) Cherodian, A.; Hughes, M.; Noirez, L.; Hardouin, F. *Liq. Cryst.* **1994**, *16*, 421–428.
(39) Ye, C.; Zhang, H. L.; Huang, Y.; Chen, E. Q.; Lu, Y. L.; Shen, D. Y.; Wan, X. H.; Shen, Z. H.; Cheng, S. Z. D.; Zhou, Q. F. *Macromolecules* **2004**, *37*, 7188–7196.
(40) Zhao, Y. F.; Fan, X. H.; Wan, X. H.; Chen, X. F.; Y, Y.; Wang, L. S.; Xia, D.; Zhou, Q. F. *Macromolecules* **2006**, *39*, 948–956.
(41) Chai, C. P.; Zhu, X. Q.; Wang, P.; Ren, M. Q.; Chen, X. F.; Xu, Y. D.; Fan, X. H.; Ye, C.; Chen, E. Q.; Zhou, Q. F. *Macromolecules* **2007**, *40*, 9361–9370.
(42) Chen, S.; Gao, L. C.; Zhao, X. D.; Chen, X. F.; Fan, X. H.; Xie, P. Y.; Zhou, Q. F. *Macromolecules* **2007**, *40*, 5718–5725.
(43) Chen, S.; Zhang, L. Y.; Gao, L. C.; Chen, X. F.; Fan, X. H.; Shen, Z. H.; Zhou, Q. F. *J. Polym. Sci., Part A: Polym. Chem.* **2009**, *47*, 505–514.
(44) Chen, X. F.; Tenneti, K. K.; Li, C. Y.; Bai, Y. W.; Zhou, R.; Wan, X. H.; Fan, X. H.; Zhou, Q. F. *Macromolecules* **2006**, *39*, 517–527.
(45) Pan, Q. W.; Chen, X. F.; Fan, X. H.; Shen, Z. H.; Zhou, Q. F. *J. Mater. Chem.* **2008**, *18*, 3481–3488.
(46) Pan, Q. W.; Gao, L. C.; Chen, X. F.; Wang, P.; Chai, C. P.; Zhou, Q. F. *Macromolecules* **2007**, *40*, 4887–4894.
(47) Yi, Y.; Wan, X. H.; Fan, X. H.; Dong, R.; Zhou, Q. F. *J. Polym. Sci., Part A: Polym. Chem.* **2003**, *41*, 1799–1806.
(48) Gao, L. C.; Pan, Q. W.; Chen, X. F.; Fan, X. H.; Zhang, X. L.; Zhen, Z. H.; Zhou, Q. F. *Macromolecules* **2007**, *40*, 9205–9207.
(49) de Genes, P. G.; Prost, J. *The Physics of Liquid Crystals*; Oxford: New York, 1993.
(50) Bracon, F.; Guittard, F.; Givenchy, E. T.; Cambon, A . *J. Polym. Sci., Part A: Polym. Chem.* **1999**, *37*, 4487–4496.
(51) Herminghaus, S. *Europhys. Lett.* **2000**, *52*, 165–170.
(52) Zhao, N.; Xie, Q. D.; Weng, L. H.; Wang, S. Q.; Zhang, X. Y.; Xu, J. *Macromolecules* **2005**, *38*, 8996–8999.
(53) Vickers, J. A.; Caulum, M. M.; Henry, C. S. *Anal. Chem.* **2006**, *78*, 7446–7452.